

CAAP Quarterly Report

Date of Report: Jan 8th 2021

Prepared for: *U.S. DOT Pipeline and Hazardous Materials Safety Administration*

Contract Number: 693JK31850008CAAP

Project Title: Fluorescent Chemical Sensor Array for Detecting and Locating Pipeline Internal Corrosive Environment

Prepared by: Dr. Ying Huang, Dr. Wenfang Sun, and Dr. Hao Wang

Contact Information: Dr. Ying Huang, Email: ying.huang@ndsu.edu, Phone: 701.231.7651

For quarterly period ending: Jan 10th 2021

Business and Activity Section

(a) Contract Activity

Discussion about contract modifications or proposed modifications:

None.

Discussion about materials purchased:

None.

(b) Status Update of Past Quarter Activities

None.

(c) Cost share activity

No cost share in this quarter.

(d) Task 2 & 3: Development of Fluorescent/Colorimetric Chemical Sensor Array for Internal Corrosive Water Detection & Corrosion Model for Corrosion Prediction

In this quarter, we continued the research efforts on three tasks: Task 2.1 Development of the Fluorescent/Colorimetric Chemical Sensor Array of Task 2 (Development of Fluorescent/Colorimetric Chemical Sensor Array for Internal Corrosive Water Detection), by developing sensor film for the H⁺/pH; Task 2.2 Calibration of of the Fluorescent/Colorimetric Chemical Sensor Array of Task 2, by analyzing sensor film characteristics and quantifying the color changes of the H⁺/pH, in addition to all other tested ions in previous quarters with the development of color maps for concentration measurements from the sensor array; and Task 3 (Corrosion Model for Corrosion Prediction), based on the laboratory tests on the corrosion rate in Sulfur, the corrosion prediction model is summarized. The detail findings are described as below.

1. Background and Objectives in the 9th Quarter

1.1 Background

This project is designed to develop passive colorimetric/fluorescent chemical sensor array for locating and detecting corrosive water inside pipes. Inside the pipelines, the transported crude oil may include a hot mixture of free water, carbon dioxide (CO₂), hydrogen sulfide (H₂S) and microorganisms. The different chemical components inside oil/water environment such as HCO₃⁻ / CO₃²⁻, Fe³⁺, S²⁻, H⁺ or pH may result in different internal corrosion mechanisms, such as sweet corrosion or sour corrosion. The passive colorimetric sensor array to be developed in this project is intended to detect the concentration changes of the five above mentioned important chemical species in the internal oil/water environment of the pipeline and use these detected environmental data to predict the internal corrosion progressing of pipelines.

1.2 Objectives in the 9th Quarter

In this quarter, the Task 2.1 was completed by developing the sensor film to detect the changes of H⁺/pH concentration and its detailed sensitivity tests were performed. The gradient color maps in addition to a specified color code for the determination of all the Fe³⁺, S²⁻, and H⁺ quantitatively were further analyzed for Task 2.2. For task 3, the corrosion prediction model was developed for steel in S²⁻ environment.

2. Results and Discussions

2.1 Development of Colorimetric/Fluorescent Chemical Sensor Array for Internal Corrosive Water Detection (Task 2.1)

2.1.1 Development of H⁺/pH sensor

In the previous reports, sensors detecting Fe³⁺ and S²⁻ had been developed and tested. In this quarter, H⁺/pH sensor (Sensor 1 in previous reports) was embedded in the selected polymer membrane developed in previous report to test the responses of the sensor film for various H⁺/pH solutions. The section describes the preparation and extraction of the chemical component for the used H⁺/pH sensor in this research. Figure 1 shows the synthetic scheme for the sensor preparation as detailed below:

- 1) The Compound **1** in Figure 1, also known as tert-butyl 2-bromo-1H-pyrrole-1-carboxylate, was produced by converting bromination of pyrrole into a 2-bromopyrrole by using NBS in THF followed by adding di-tert-butyl decarbonate, triethylamine, and DMAP to protect the NH reacting site.
- 2) The Compound **2** in Figure 1, tert-butyl 2-(2-methoxyphenyl)-1H-pyrrole-1-carboxylate, was prepared by reacting Compound **1** with 2-methoxyphenylboronic acid via Suzuki coupling reaction.
- 3) In the presence of NaOMe, Compound **2** was deprotected, resulting in Compound **3** in Figure 1.
- 4) Meanwhile, Suzuki coupling reaction between 4-iodobenzaldehyde and (4-(diphenylamino)phenyl)boronic acid produced Compound **4** in Figure 1, the 4'-(diphenylamino)-[1,1'-biphenyl]-4-carbaldehyde.
- 5) Condensation reaction of Compounds **3** and **4** followed by oxidation reaction gave the desired H⁺/pH sensor (Sensor 1) in this research, which is the (Z)-4'-((5-(2-methoxyphenyl)-1H-pyrrol-2-yl)(5-(2-methoxyphenyl)-2H-pyrrol-2-ylidene)methyl)-N,N-diphenyl-[1,1'-biphenyl]-4-amine. Figure 2 shows the chemical structure of the final H⁺/pH sensor.

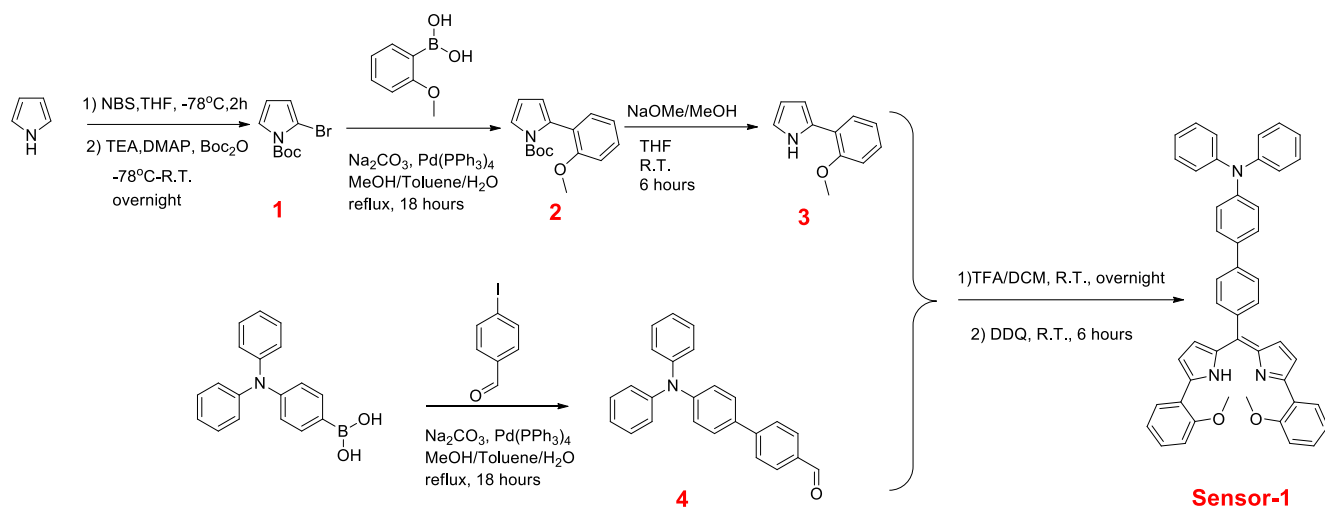


Figure 1 Synthetic scheme for H^+ /pH sensor.

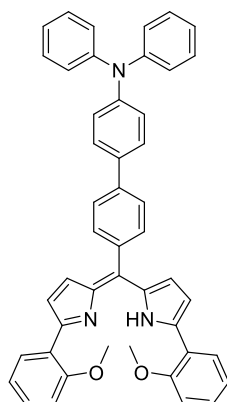


Figure 2 Chemical structure of the H^+ /pH sensor.

Figure 3 (a) shows the resulted H^+ /pH sensor in powder based on the above procedures which is in dark red color and Figure 2 (b) is the H^+ /pH sensor diluted in DI water, which shows pink-red color.

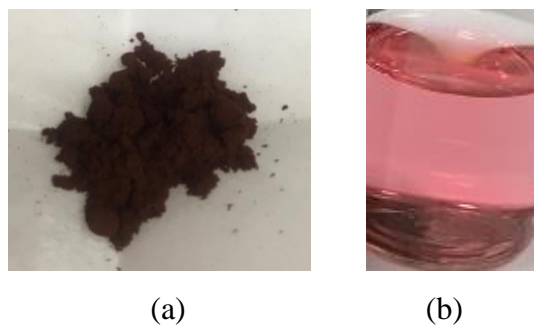


Figure 3 The H^+ /pH sensor (a) powder and (b) liquid

2.1.2 Colorimetric response of the H^+ /pH sensor in solution environment

To test the colorimetric responses of the H^+ /pH sensor for detecting pH changes, the sensors were placed in the solution of various pH environments and the color changes were recorded and compared. According to the PH indicator paper, three different PH of designed aqueous solutions were intended to be prepared: PH=2, PH=4, PH=6. However, when preparing the solution, the actual pH varied from the pH indicator paper as shown in Table 1, which were 1.98, 4.19, and 5.56.

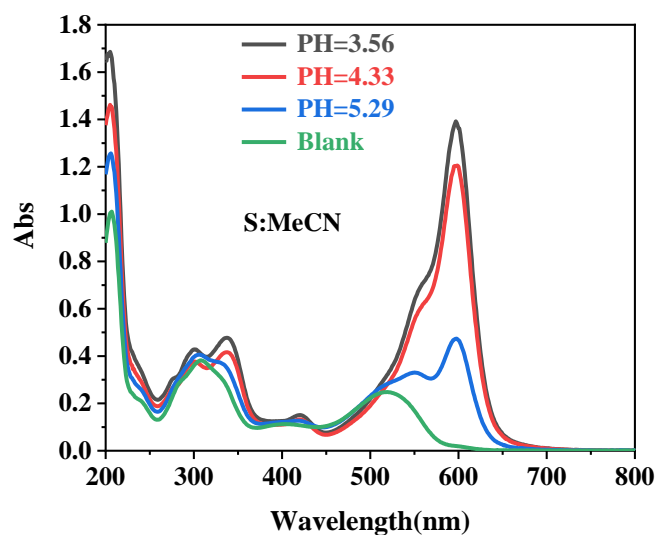
Table 1 pH value of dissolved H⁺/pH sensor

Designed aqueous solution PH	2	4	6
Actual aqueous solution PH	1.98	4.19	5.56
Sample actual PH	3.56	4.33	5.29

Meanwhile, the solution of the H⁺/pH sensor was also prepared in acetonitrile with concentration of 1mg in 100 ml acetonitrile. Four 20 ml vials of 10 ml sensor solution were prepared. One drop of the designed pH aqueous solutions and one drop of water were added into the four prepared sensor vials. Obvious color changes were observed as shown in Figure 4 (a). As the pH decreased, the color of the sensor solution turned from pink, to purple, and further to blue. The color changed with different H⁺ concentrations. After the experiments, the pH values of the sensor solutions were also measured by the digital PH meter, as also shown in Table 1. Compared with the original pH of the sensor solution of 4.0, the pH of the sensor solutions also varied by adding solutions with different pH values.



(a)



(b)

Figure 4 H⁺/pH sensor color changes (a) and UV chart (b) when adding acidic solutions with different pH

Figure 4 (b) further shows the UV-vis spectrum of the sensors after adding acidic solutions with different pH. It can be clearly seen that with the pH value decreased (the acidic increased), the max absorption wavelength showed obvious red shift and intensity also increased. The blue curve (pH=5.29) showed a transition status the solution color also turned a transitional color.

2.1.3 Fabrication of polymer membrane embedded with H^+ /pH sensor

The mixing procedure of the polymer membrane was similar described in previous reports with some adjustments to better fit this sensor. Since the developed H^+ /pH sensor powder can only be dissolved in organic solution, the dosage of organic solution changed. The detailed fabrication of the membrane followed four steps as below:

- 1) Solution A: Cellulose acetate (CA) (1 g) was dissolved in DMF (8 g) and hexane (3 g), stirring at 85 °C for 2 h to form a homogeneous casting solution. Then the mixture was moved to room-temperature-stirring until the next mixing procedure.
Solution B: Poly (methyl methacrylate) (PMMA) (1g) was dissolved in THF (6 mL) and the PMMA solution was stirred at room temperature for 24 h to make it completely homogeneous.
- 2) The polymer solutions A and B were mixed together and stirred at 85 °C for 1h to form a homogenous phase.
- 3) 0.1 mg H^+ /pH sensor powder was added into the polymer mixture. While the solution was kept stirred for another 30 min.
- 4) Pour a thin film on a glass plate and put it inside a hot chamber at 85 °C for 1 h until hardened. The film was then covered by a glass container and left at room temperature for 10 min for cooling down.
- 5) The film was then immersed in a room-temperature DI water coagulation bath until it was detached from the holder. The film was taken out and kept in another fresh DI water for 48 h to remove any trace of solvent. The wet film was used directly for the tests.

2.1.4 Colorimetric responses of the H^+ /pH sensor films in various pH environments

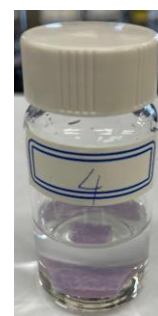
The fabricated thin sensor film was casted and cut into pieces for color-response test in acid-to-neutral solutions as shown in Figure 5 (a). The fabricated sensor films were then immersed in acid-to neutral solution ranged from 2 to 7 for 24h to observe the color changes of the sensor films, which are shown in Figure 5 (b). An obvious color change was observed.



Target pH 2
Tested pH 1.98



Target pH 3
Tested pH 3.14



Target pH 4
Tested pH 3.86

(a) H⁺/pH Sensor film



Target pH 5
Tested pH 5.32



Target pH 6
Tested pH 6.76



Target pH 7
Tested pH 6.93

(b) Samples in solution

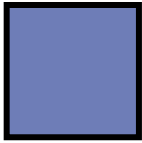
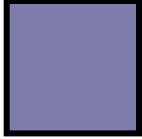
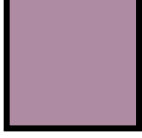
Figure 5 Example of the fabricated sensor films and color changes of the sensor films in different pH environments

2.2 Calibration of the Fluorescent/colorimetric Chemical Sensor Array (Task 2.2)

2.2.1 Quantitative analysis of colorimetric H⁺/pH sensor

The color changes of the H⁺/pH sensor films towards different pH solutions were further analyzed following the same procedures described in previous reports to create the color change contour map. The representative colors under each tested pH are shown in Table 2. It is clearly observed the embedded sensor had significant response to concentration of H⁺ ions in the solution, which turned the sensor film from original color, which was light red to blue as the pH decreased. In the acidic zone of the pH development, the sensor film showed blue shifts characteristics.

Table 2 Color shifts and representative color of H⁺/pH sensor films under different pH solutions

pH	Tested pH	Sample appearance	Representative color	RGB value	Yxy Value
2	1.98			110, 125, 183	21.5, 21.0, 36.0
3	3.14			126, 124, 173	22.8, 21.6, 32.1
4	3.86			174, 139, 163	33.6, 30.1, 29.3

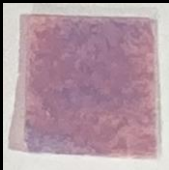
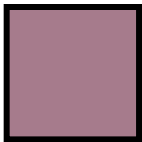
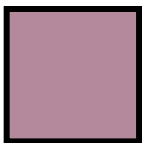
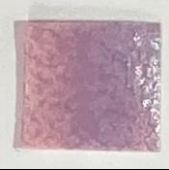
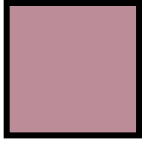
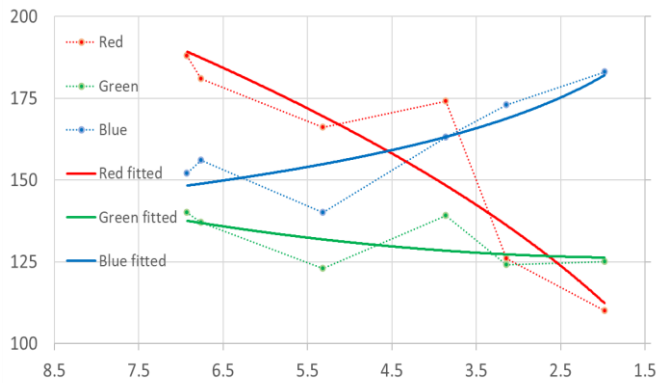
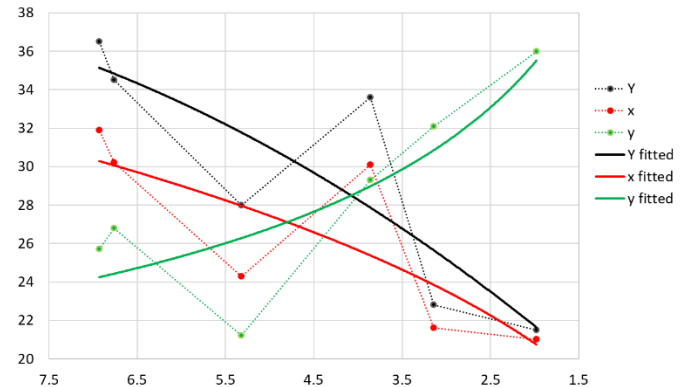
5	5.32			166, 123, 140	28.0, 24.3, 21.2
6	6.76			181, 137, 156	34.5, 30.2, 26.8
7	6.93			188, 140, 152	36.5, 31.9, 25.7

Figure 6 (a) shows the RGB changes with different pH values. As the pH decreased, the color changed from light red to light blue. In specific, the green portion of the color dropped slightly, while in general it kept a steady trend. The red portion decreased rapidly, while on the contrary, blue increased to the same degree of red. This indicated that when in the pH decreased, the red portion was replaced by blue, when the green portion kept stable. Figure 6 (b) shows the Yxy value changes with various pH values. The x and y showed opposite develop trend as red decreased and y increased, and their amplitudes kept the same. However, Y value which represents the brightness of the color decrease significantly when the acidity develops.



(a) RGB vs pH



(b) Yxy values vs pH

Figure 6 RGB (a) and Yxy value (b) change of pH sensor

2.2.2 Quantitative analysis of colorimetric responses for all sensor films on the sensor array

Based on our last quarterly report, the color map of the S^{2-} and Fe^{3+} ions were previously developed, however, they showed discontinuity from intuitive observation. Thus, further optimized analysis of the contour map for all the three sensor films on S^{2-} , Fe^{3+} , and pH were performed in this quarter by using the Linear Gradient Difference Theory. The linear gradient (also axial gradient) [1] varies along the axis between two defined endpoints. All points on a line perpendicular to the axis have the same color value. On the other hand, the radial gradient varies radially along the axis between two defined ends, which is

usually a circle. If the point is located on the circumference of a circle where the center point falls on the axis, the points share the same color value. The radius of the circular portion of the gradient is defined by the radius of the end circle and the radius of each intermediate circle varies linearly from one end to the other. According to this theory, when two colors A and B with specific color code determined as shown in Figure 7, any point M in the middle works as transmitting color representatively to get middle points in the color chart. To determine the middle point M, which is also called floating color, the color code of M can be divided into several steps with step depth as t, which can be calculated as:

$$t = |AM|/|AB| . \tag{Eq.1}$$

As $|AM| \geq 0$, and $|AM| \leq |AB|$, thus $t \in [0, 1]$, when the length of $AB = l$, the x and y values can be calculated as:

$$x = x_1 + t * l , \tag{Eq.2}$$

$$y = y_1 + t * l . \tag{Eq.3}$$

By the setting of cyclic calculation in Matlab, any points on line AB can be calculated from Eq.4 as:

$$\begin{aligned} & \text{for (float } t = 0.0; \text{ rate} \leq 1.0; t += 0.1) \\ & \{x = x_1 + t * l; \quad y = y_1 + t * l;\} . \end{aligned} \tag{Eq.4}$$

which can be understood as a gradual change of coordinates. The x and y components of the coordinates are changed. The color gradation is theoretically the same, except that the three components of R, G, and B are changed. If the coordinates and colors (r1, g1, b1), (r2, g2, b2) of points A and B are known at the same time, then the coordinates and colors of point M can be obtained as [2]:

$$\begin{aligned} & \text{for (float } t = 0.0; \text{ rate} \leq 1.0; t += 0.1) \\ & \left\{ \begin{aligned} & r = r_1 + t * (r_2 - r_1); \\ & g = g_1 + t * (g_2 - g_1); \\ & b = b_1 + t * (b_2 - b_1) \end{aligned} \right\} . \end{aligned} \tag{Eq.5}$$

In other words, if you know the t corresponding to a certain point, then you can calculate the color of this point. As shown in Figure 8, to fill the rectangle along AB, the coordinates and colors of points A and B are known, and the coordinates of any point N in the rectangle are also known (cycle through all points in the rectangle), then you can Find the projection M of point N on AB (MN is perpendicular to AB), $t = |AM|/|AB|$, use Eq. 5 to find the color of point M, the color of point M is the color of point N.

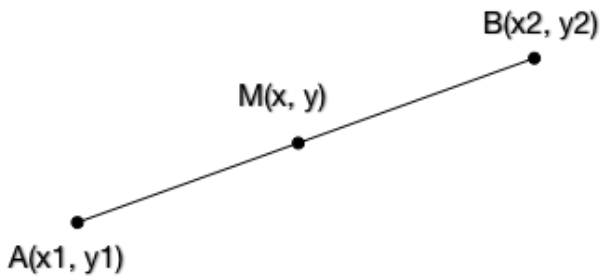


Figure 7 Example of middle point color

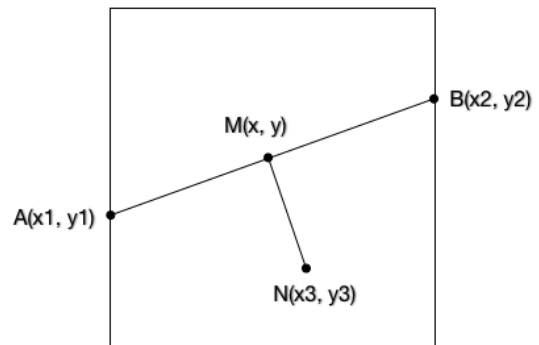


Figure 8 Middle point calculation on 2-D expansion plane

For the vertical gradient in Figure 8, point A (x1, y1) is the upper left corner of the rectangle, point B (x2,

y2) is the sitting corner of the rectangle, and any point N (x, y) in the rectangle is on AB. The coordinates of the projection M are (x1, y), so $t = (y-y1)/(y2-y1)$. When knowing t, the corresponding color can be obtained.

In this research, the axial of the color shift should be along the changing direction of ion concentration and pH changes, which represents the y axis in all color maps. The defined end points were selected in the original color map of Fe^{3+} and S^{2-} ions shown in Figure 9. Thus, three times of inner gradient in MATLAB were done to improve the color map for a natural and uniform transforming gradient color. In addition, by using the same treatment, color map of pH was produced at acidic side of the solution environment between pH from 2 to 7. Figure 10 (a~c) showed the optimized color contour maps for all the three ions.

From the concluded color chart of Fe^{3+} , S^{2-} and acidic pH environments, there are several features worth mentioning:

- For both of the Fe^{3+} and S^{2-} ion environments, the colors of the sensor films show minor changes under low concentration condition ($\leq 0.1\%$). However, when the concentration increases, the obvious color changes can be observed from light to thick representative colors.
- For the Fe^{3+} and S^{2-} sensors, when the concentration exceeds 0.9%, majority of reactive particles have experienced complex reaction which makes the sensor film fully colored, indicating that the maximum detection concentration is 0.9%.
- For the pH sensors, the color chart only represents the changes under acidic condition. The reason of the absence of alkaline condition is that buffer solution is necessary during the fabrication process of the sensor film. However, one little drop of the alkaline can induce the sensor film to experience high pH value before they are immersed into real alkaline solution. Thus, before the exact quantity of alkaline used in fabrication, which is our current work focus, the results can be inaccurate due to residual OH^- . The alkaline section will be done in the following report period.

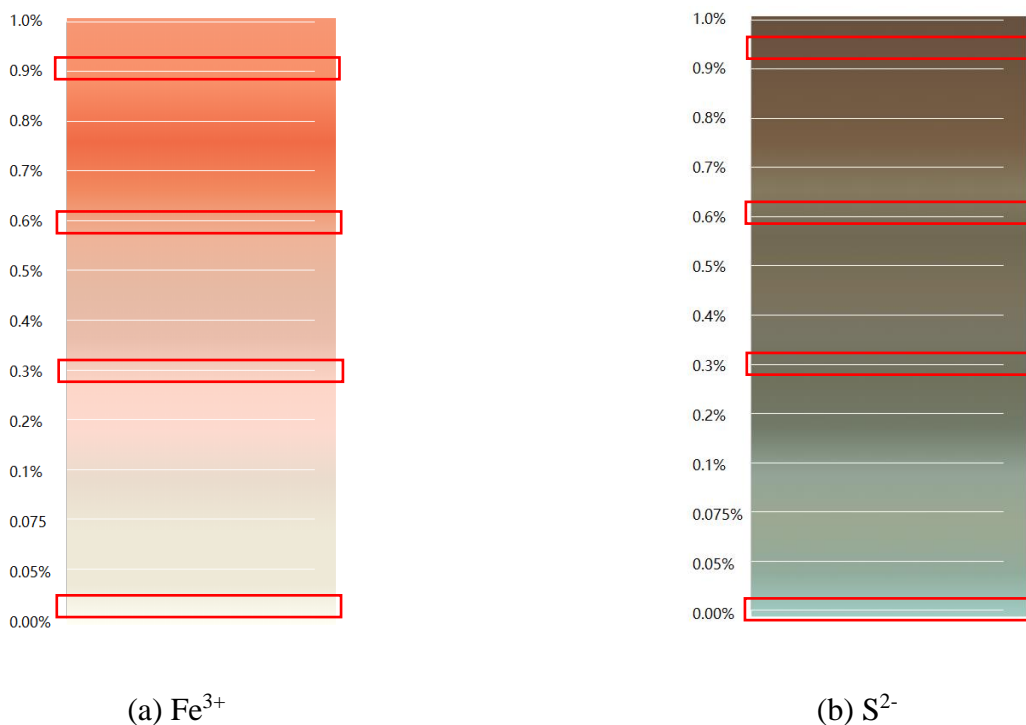


Figure 9 Gradient color chart of Fe^{3+} (a) and S^{2-} sensor (b)

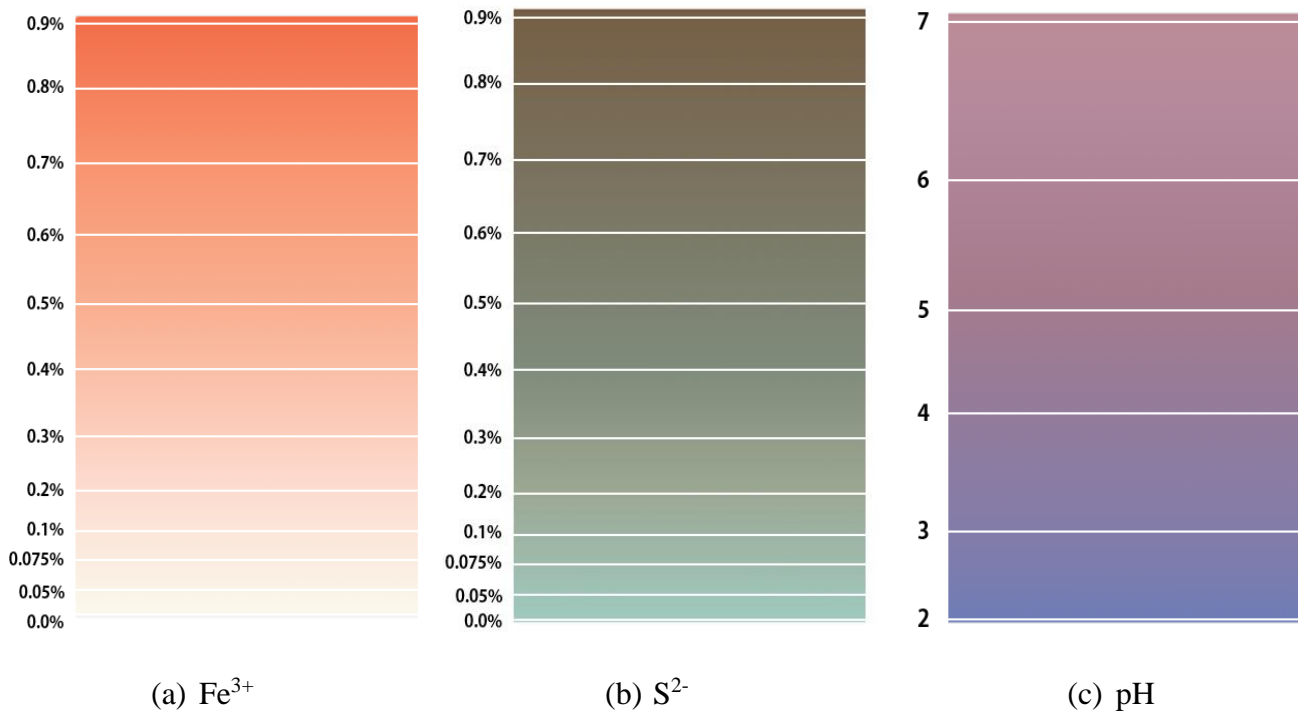


Figure 10 Optimized color contour map of Fe^{3+} (a), S^{2-} (b), and color map for pH detection (c)

2.3 Integration of Corrosive Water into Internal Corrosion Prediction Models (Task 3)

In the last quarter, potentiodynamic tests were performed to obtain the corrosion rate of steel under the present of S^{2-} ions. In this quarter, more tests were done to achieve the corrosion model of corresponding ions. The test instruments and settings are shown in Figure 11 and the tested data are shown in Table 3 with calculated corrosion rate following Eq. (6) below:

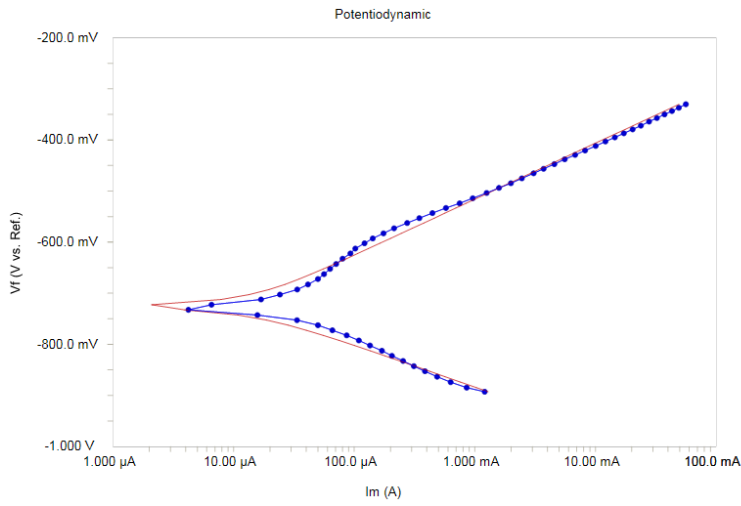
$$CR = \frac{I_{\text{corr}} K \cdot EW}{dA} \quad (\text{Eq.6})$$

in which, I_{corr} is the corrosion current in amp, K is constant defines the unites for the corrosion rate. The value is 3272 if use mm/year (mmpy), and is 1.288×10^5 if use milli-inches/year (mpy), EW is the equivalent weight in grams/equivalent, d is the density in g/cm^3 , and A is the sample area in cm^2 .

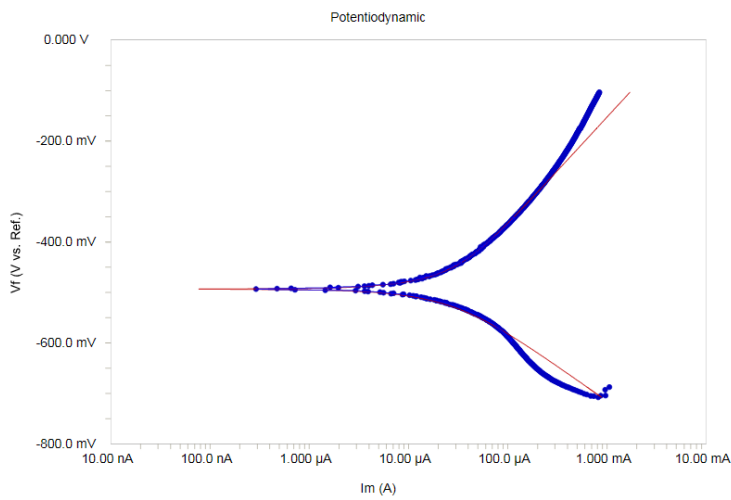


Fig. 11 Test instruments

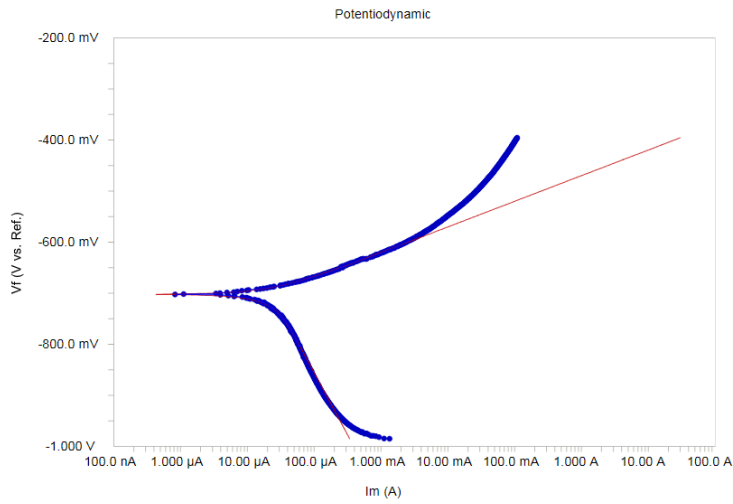
Table 3 Test results with Tafel fitting and calculated corrosion rate



3.5% NaCl, 0.00% S²⁻
 Initial E (V): -0.3 vs. Eoc
 Final E (V): 0.3 vs. Eoc
 Scan Rate (mV/s): 1 Sample Period (s): 1
 Sample Area (cm²): 1
 Density (gm/cm³): 7.87
 Equiv. Wt: 1 IR
 Time(s): 1800 Stab.(mV/s): 0
 BetaA (V/decade): 0.1097
 BetaC (V/decade): 0.0824
 Icorr (A): 0.0000122
 Ecorr (V): -0.726
 Corrosion Rate (mmpy): 5.07519432E-2



3.5% NaCl, 0.01% S²⁻
 Initial E (V): -0.3 vs. Eoc
 Final E (V): 0.3 vs. Eoc
 Scan Rate (mV/s): 1 Sample Period (s): 1
 Sample Area (cm²): 1
 Density (gm/cm³): 7.87
 Equiv. Wt: 1 IR
 Time(s): 1800 Stab.(mV/s): 0
 BetaA (V/decade): 0.632
 BetaC (V/decade): 0.0575
 Icorr (A): 0.0000128
 Ecorr (V): -0.822
 Corrosion Rate (mpy): 5.31251414E-2



3.5% NaCl, 0.05% S²⁻

Initial E (V): -0.3 vs. Eoc

Final E (V): 0.3 vs. Eoc

Scan Rate (mV/s): 1 Sample Period (s): 1

Sample Area (cm²): 1

Density (gm/cm³): 7.87

Equiv. Wt: 1 IR

Time(s): 1800 Stab.(mV/s): 0

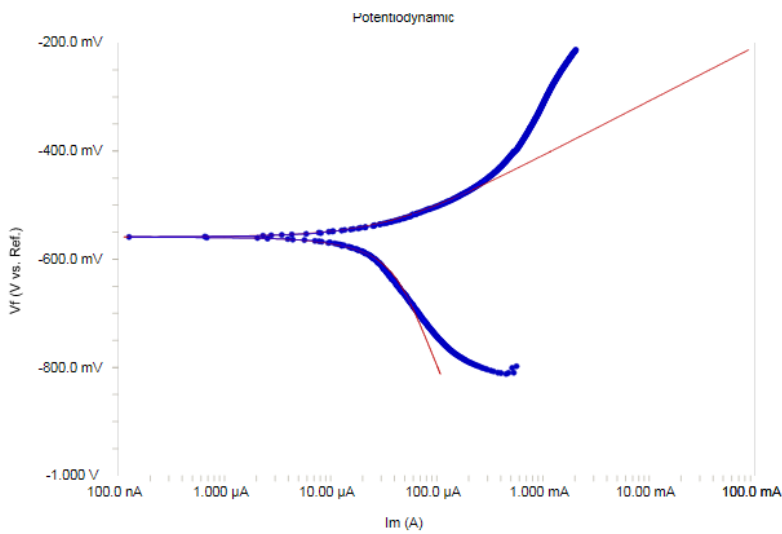
BetaA (V/decade): 0.0502

BetaC (V/decade): 0.2438

Icorr (A): 0.0000235

Ecorr (V): -0.702

Corrosion Rate (mpy): 9.77029288E-2



3.5% NaCl, 0.10% S²⁻

Initial E (V): -0.3 vs. Eoc

Final E (V): 0.3 vs. Eoc

Scan Rate (mV/s): 1 Sample Period (s): 1

Sample Area (cm²): 1

Density (gm/cm³): 7.87

Equiv. Wt: 1 IR

Time(s): 1800 Stab.(mV/s): 0

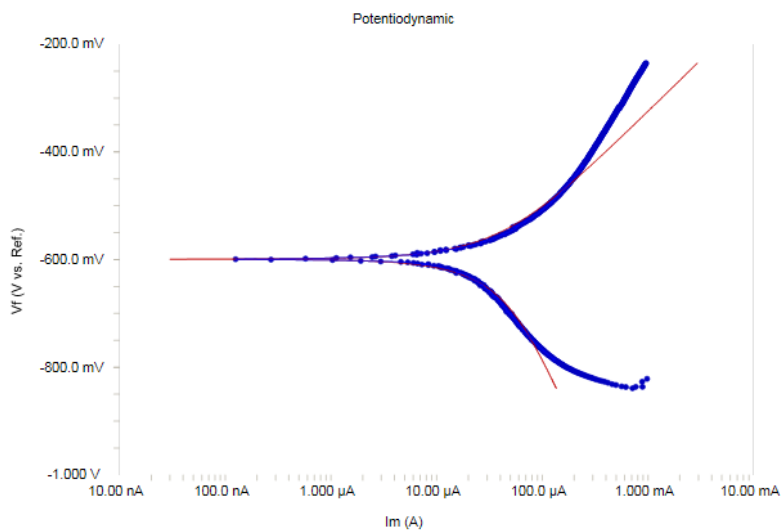
BetaA (V/decade): 0.1021

BetaC (V/decade): 0.3745

Icorr (A): 0.000019

Ecorr (V): -0.743

Corrosion Rate (mpy): 7.89472386E-2



3.5% NaCl, 0.25% S²⁻

Initial E (V): -0.3 vs. Eoc

Final E (V): 0.3 vs. Eoc

Scan Rate (mV/s): 1 Sample Period (s): 1

Sample Area (cm²): 1

Density (gm/cm³): 7.87

Equiv. Wt: 1 IR

Time(s): 1800 Stab.(mV/s): 0

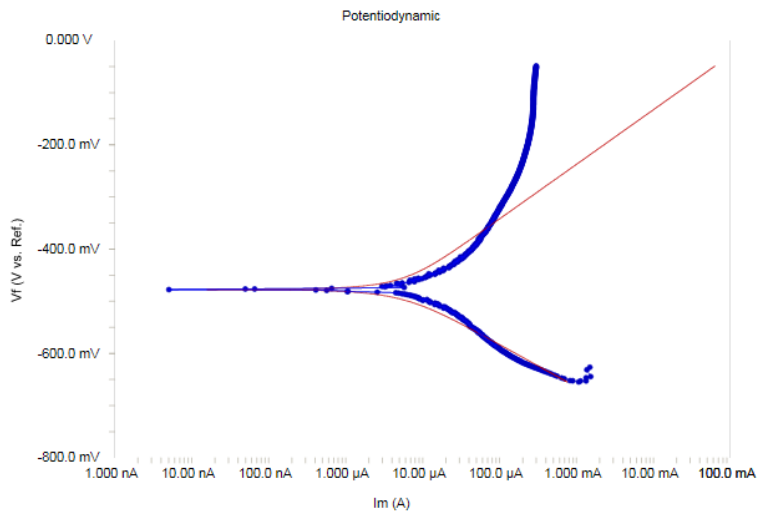
BetaA (V/decade): 0.1924

BetaC (V/decade): 0.4263

Icorr (A): 0.0000377

Ecorr (V): -0.599

Corrosion Rate (mmpy): 0.1670412



3.5% NaCl, 0.5% S²⁻

Initial E (V): -0.3 vs. Eoc

Final E (V): 0.3 vs. Eoc

Scan Rate (mV/s): 1 Sample Period (s): 1

Sample Area (cm²): 1

Density (gm/cm³): 7.87

Equiv. Wt: 1 IR

Time(s): 1800 Stab.(mV/s): 0

BetaA (V/decade): 0.1047

BetaC (V/decade): 0.0817

Icorr (A): 0.0000511

Ecorr (V): -0.617

Corrosion Rate (mmpy): 0.3470412

Based on the literature review, the corrosion prediction model was previously developed following the numerical model derivation by Greco and Wright [3] and Sardisco, et al., [4], which predicts the corrosion rate with the consideration of H⁺, S²⁻ and dissolved O₂ under moist environment. They found out that a protective sulfide film formed at concentrations of H₂S < 1,700 ppm corresponding to gas pressure of < 0.1 psia. In addition, Ho-Chung-Qui [5] and Williamson reported that, in an environment containing H₂S/CO₂ at the ratio of ~ 4, chloride concentration > 10,000 ppm caused severe localized corrosion. The corrosion was associated with the presence of ferrous chloride (FeCl₂), which formed as a layer between iron sulfide and the metal. Thus, the corrosion rate prediction model could be represented as a function of these corrosion-inducing factors as Eq. 7:

$$CR = 8.7 + 9.86 \times 10^{-3}(O_2) - 1.48 \times 10^{-7}(O_2)^2 - 1.31(pH) + 4.93 \times 10^{-2}(CO_2)(H_2S) - 4.82 \times 10^{-5}(CO_2)(O_2) - 2.37 \times 10^{-3}(H_2S)(O_2) - 1.11 \times 10^{-3}(O_2)(pH) \quad (\text{Eq.7})$$

In next quarter, we will use our experimental data in Table 3 and previous reports to update the above corrosion model to with appropriate coefficients in Eq. (7) for the influence of S²⁻ to the corrosion rate of steel.

2.3 Student Mentoring

There are six graduate students (Xinyang Sun, Ph. D. in Chemistry at NDSU, Shuomang Shi and Ratna Divya Yasoda, two Ph. D. students in Civil and Environmental Engineering at NDSU, Salman Ahmad and Tofatun Jannat, two Masters students in Civil and Environmental Engineering at NDSU, and Wei Sun, PhD student from RUNB Civil Dept.) worked on this project. Due to the increasing risk of lab work, no undergraduate assistants were hired during this quarter or next quarter. Undergraduate research assistants will resume working for this project in Summer and Fall 2021 if it is deemed to be safe for them to work in the lab environments.

2.4 Future work

In the 10th quarter, we will continue working on all tasks specifically as:

- 1) Task 2: Test pH above 7 and further optimize the color map;
- 2) Task 3: Further include the input for the corrosion model from the sensor array color map into the corrosion prediction model;
- 3) Task 4: Use the robot kits for laboratory tests for the sensor array as validation and optimization.

References:

- [1] CSS Image Values and Replaced Content Module Level 3. W3C Candidate Recommendation. 2012-04-17
- [2] Asente, Paul; Carr, Nathan, Creating contour gradients using 3D bevels, Proceedings of the Symposium on Computational Aesthetics (CAE '13, Anaheim, California), New York, NY, USA: ACM: 63–66, 2013, ISBN 978-1-4503-2203-4, doi:10.1145/2487276.2487283
- [3] E.C. Greco, W.B. Wright, Corrosion 18: p. 119t-124t.
- [4] J.B. Sardisco, W.B. Wright, E.C. Greco, Corrosion 19 (1963): p. 354t.
- [5] D.F. Ho-Chung-Qui, A.I. Williamson, “Pipeline Corrosion—H₂S and O₂ Corrosion of Pipelines,” Corrosion Information Compilation Series (Houston, TX: NACE International, 1999), p. 41.